Geometrical and Vibrational Properties of Nucleic Acid Constituents Interacting with Explicit Water Molecules as Analyzed by Density Functional Theory Calculations. 1. Uracil + $n_w H_2O$ (n_w = 1,...,7)

Marie-Pierre Gaigeot and Mahmoud Ghomi*

Laboratoire de Physicochimie Biomoléculaire et Cellulaire, UPRESA CNRS 7033, Case courrier 138, Université Pierre et Marie Curie, 4 Place Jussieu, F-75252 Paris Cedex 05, France

Received: October 31, 2000; In Final Form: February 14, 2001

To analyze the preferential sites of interaction of water molecules with uracil (RNA base) through the first hydration shell, we resorted to density functional theory (DFT) calculations by means of B3LYP exchange and correlation functionals. The effect of two different basis sets with and without diffuse orbitals, i.e., 6-31G* and 6-31++G*, respectively, has been studied on the energetics, as well as on the geometrical and vibrational properties, of the studied compounds. Water molecules have been gradually placed in an average plane containing uracil, and their number (n_w) was varied from 1 to 7. For a given value of n_w, different possible interaction sites of water molecule(s) with respect to the base have been taken into consideration. The results obtained from this investigation allowed us to estimate the energy difference separating optimized configurations by taking into account both electronic and vibrational energies. The most energetically favorable configurations for a given n_w value were then used in further calculations with higher n_w values. It has been shown that the most energetically favorable supermolecular configurations found with large number of n_w contain water dimers and water trimers. Geometrical parameters of uracil, water molecules, and hydrated uracil have been discussed in detail. Calculated vibrational modes for uracil and hydrated uracil (uracil + $7H_2O$) have been compared with those previously analyzed by optical spectroscopy.

I. Introduction

Water is the natural medium of biological molecules participating in different processes involving living cells. In particular, several structural features that are necessary for the biological functions of nucleic acids, such as double helix formation in DNA or chain folding in RNA, depend on the interactions with surrounding water. The hydration of nucleic acids is controlled by the interaction of water molecules with various hydrophilic sites such as phosphates, bases, and sugars.[1−5] Previous studies of X-ray diffraction patterns have clearly shown that an average number of 20 water molecules is necessary to adequately represent the first hydration shell of a nucleotide (base+sugar+phosphate).[1,2] These experimental studies, generally performed on short size molecular motifs such as dinucleoside-monophosphate, trinucleoside-diphosphates, tetradecamers, or on larger oligonucleotide systems, have revealed that in nucleic acids, phosphate groups and bases are more hydrated than sugars.[6]

It is a matter of fact that in double helix regions of nucleic acids the donor and acceptor sites of the bases are mainly involved in interbase hydrogen bond networks. However, during the base-pair opening process,[7,8] surrounding water molecules can interact with nucleic acid bases through major and minor grooves. On the other hand, in particular nucleic acid structures, such as bulges, internal loops and loops, nonpaired bases can interact directly with water.[9−12]

Among theoretical calculations, only those based on quantum mechanical approaches can yield precise information on the energetics and geometrical and vibrational properties of the supermolecules formed by a host molecule surrounded by explicit water. A series of quantum mechanical investigations have been performed up to now on the hydration of the nucleic acid base that are from the chemical point of view of conjugated heterocycles. Because of the chemical structure of the bases, the majority of H-bond interactions with water are of the following types: C═O···H(W), N−H···O(W), and N···O−H(W), where W stands for a water molecule. However, weaker H-bond interactions of C−H···O(W) type should also be considered as important structural stabilizing factors upon nucleic acid−water interactions.[13−15] Because of the simple chemical structure of uracil (RNA base), the theoretical analysis of its hydration has received a great deal of attention during the past years. Among these previous works, one can recall those devoted to the uracil + $1H_2O$ complex performed at the HF,[16,17] MP2,[18,19] DFT,[20,21] and MBPT[22] levels, as well as those on uracil + $2H_2O$ at the DFT level.[23,24] Only one publication has reported the interaction of uracil with three water molecules (n_w = 3) at the HF level, accompanied with a few single point estimations at the MP2 level.[25] It was then concluded[25] that the first hydration shell of uracil is complete with only three water molecules. A recent paper,[26] based on a joint use of ab initio calculations and electrostatic potential mapping, reports a more detailed analysis of uracil hydration with n_w = 1, 2, 4, 6, 10, 12, 15. This analysis has been performed mainly at the HF/6-31G** level, where the attention was focused mostly on the three-dimensional solvation of uracil, and especially on the hydrogen bond network formed by water molecules located in- and out-of the uracil plane. As a conclusion, no systematic investigation of the uracil−water interaction as a function of increasing n_w values is available in the literature.

* To whom all correspondence should be addressed. Phone: +33−1−44277555. Fax: +33-1-44277560. E-mail: ghomi@lpbc.jussieu.fr

10.1021/jp0040401 CCC: $20.00
Published on Web 05/05/2001

In this report, our aim is to systematically analyze, at the DFT level, the most favorable configurations of uracil + n_wH_2O complexes with water molecules basically located in an average plane including uracil. This study will lead us to (i) test the reliability of our calculations by checking again the most suitable interaction sites of one water molecule with uracil; (ii) achieve the construction of the first hydration shell in the plane of uracil by gradually increasing n_w; (iii) and to verify whether $n_w = 3$ is an optimal number for this purpose as claimed previously.[25] In the present work, the gradual increase of n_w will give us the opportunity to achieve the most energetically favorable configurations of uracil + n_wH_2O complex from the knowledge of those corresponding to uracil + $(n_w - 1)H_2O$ complex. Moreover, at each step of our investigations, vibrational calculations of uracil + n_wH_2O complexes have been undertaken at the DFT level in order to check whether the optimized configurations correspond to energy minima, and also to estimate more precisely their energy order. The reliability of these calculations will be confirmed in the light of a comparison between theoretical and observed vibrational spectra.

II. Theoretical Details

To select the theoretical method employed in the present work, we took advantage of our recent ab initio calculations on isolated nucleic acid constituents, such as bases,[27,29] phosphate,[30] ribonucleosides[30−32] and ribonucleotides,[30] at either the MP2 or DFT level of theory. We have shown in detail that DFT and MP2[32,33] levels of theory give similar results as far as the geometrical and vibrational features of nucleic acid bases are concerned. In contrast, the Hartree−Fock method provides poor results, in particular for the vibrational modes of these constituents, because of the neglect of the electronic correlation effect in this theoretical approach.[30] Hence, to analyze the present molecular compounds, the DFT method has been adopted as an excellent compromise between computational cost and involvement of electronic correlation.

All quantum mechanical computations have been performed on NEC supercomputers or on IBM workstations using the GAUSSIAN98 package.[34] Theoretical calculations have been performed at the DFT level by means of the B3LYP nonlocal exchange-correlation functional.[35] To analyze the effect of the basis set extension on both geometry and vibrational modes of molecular or supermolecular configurations, two different split valence Gaussian basis sets, i.e., 6-31G* and 6-31++G*, have been employed. In the case of uracil + n_wH_2O ($n_w = 1, 2$) complexes, the whole calculations are performed with both basis sets. For n_w values ≥ 3, geometry optimization has been first performed with 6-31G* basis set in order to compare the electronic energies of the different configurations. Then, both geometry optimization and vibrational calculations have been carried out by means of the 6-31++G* basis set.

Full geometry optimization results allowed us to obtain the electronic (E_e) and geometrical parameters. Various configurations corresponding to a given n_w value are obtained by moving the water molecules around the donor and acceptor sites of uracil (U), and are named as U$n_w - k$, where the integer k denotes one of the configurations corresponding to a given n_w. The value of k increases with the relative energy of the configuration to which it corresponds. Prime notation (′) has been used with a given k value when the topological difference between two configurations is the orientation of one water molecule with respect to uracil, the number of hydrogen bonds being kept unchanged.

Harmonic vibrational calculations performed after full geometry optimization permitted the assignment of the optimized geometry to an energy minimum by the absence of any imaginary frequency and gives the estimation of the so-called zero point vibrational energy (ZPVE), i.e., $E_v = \sum_{i=1}^{3N-6} 1/2\ h\nu_i$, where h is the Planck constant and ν_i represents one of the $3N - 6$ vibrational frequencies of the molecular compound with N atomic centers. To order the energy of uracil−water supermolecules (for a given n_w value), both electronic energy (E_e) and total energies ($E_t = E_e + E_v$) have been used. ΔE_e (ΔE_t) values of different configurations corresponding to a given uracil−water complex (uracil + n_wH_2O) are calculated with respect to the lowest energy one for which ΔE_e (ΔE_t) values are set to zero.

The effect of basis set superposition error (BSSE) has been analyzed only on uracil + $1H_2O$ configurations by means of the counterpoise method.[36] Correspondingly, the binding energy of uracil (U) to a water molecule (W), i.e., ΔE_e^{UW}, has been determined by[37]

$$\Delta E_e^{UW}(U,W) = E_e^{UW}(U,W) - E_e^{U}(U,W) - E_e^{W}(U,W)$$

where $E_e^{UW}(U,W)$, $E_e^{U}(U,W)$, and $E_e^{W}(U,W)$ are the electronic energy of uracil−water complex, uracil, and water, respectively. (U,W) means that these three contributions are estimated in the basis set used for the uracil−water complex calculations. In the corrected binding energy estimation, neither the ZPVE (E_v) nor the deformation energies for uracil and water have been taken into consideration, because of their small contribution compared to the electronic energies.

The assignments of the vibrational modes have been made by means of the potential energy distribution (PED) as calculated on the basis of internal coordinates with our homemade package (BORNS).

III. Results and Discussion

III.1. Geometry Optimization and Energy Values. Isolated Uracil, Isolated Water (water monomer), and Water Dimer. Energy values of these compounds are mentioned in Table 1, and their geometrical parameters (bond lengths and angles) are reported in Table 2 (See Figure 1 for graphical representation). Recent geometry optimizations of uracil at the MP2/6-31G*[23,24,27] and MP2/6-311G*[18] levels provide geometrical data that are very close to those estimated at the DFT level (present work). Both of the used basis sets, i.e., 6-31G* and 6-31++G*, provide a planar uracil (C_s symmetry) with geometrical parameters in agreement with those observed by X-ray[38] or electron diffraction[39] (Table 2). On the other hand, a detailed report[40] has also shown that MP2 and DFT/B3LYP calculations give similar geometrical results as far as the water monomer and water dimer are concerned. It has also been shown[40] that the observed value of the distance between the two water dimer oxygens[41] ($d_{O\cdots O} = 2.946$ Å) can never be reached by ab initio calculations, regardless of the theoretical level (DFT or MP2). It has been concluded that only upon the use of highly extended atomic basis sets can the calculated value of the above-mentioned distance get closer to the observed value.[40]

From the topological point of view, it should be mentioned that there are two different manners by which to form hydrogen bonds between two water molecules in a water dimer. This leads to two distinct configurations, namely, *linear* and *cyclic* dimers, respectively.[42] The linear dimer is stabilized by only one O−H(W1)···O(W2) hydrogen bond interaction, whereas two H-bonds of this type exist in a cyclic dimer. On the basis of spectroscopic evidences, the formation of a cyclic dimer seems to be quite improbable.[42] We have attempted to confirm this

TABLE 1: Calculated Energy Data for the Analyzed Molecular Compounds Obtained at the DFT/B3LYP Level[a]

	B3LYP/6-31G*					B3LYP/6-31++G*				
compound	E_e[b]	ΔE_e	E_v[b]	ΔE_t[c]	E_d[d]	E_e[b]	ΔE_e	E_v[b]	ΔE_t[c]	E_d[d]
uracil (U)	−414.808042		54.86			−414.830729		54.69		
water monomer	−76.407023		13.26			−76.421407		13.19		
water dimer	−152.826619		28.84		−7.88 (−5.55)	−152.853179		28.96		−6.50 (−5.30)
uracil + $1H_2O$										
U1−1	−491.238183	0.00 (0.00)	70.62	0.00	−14.51 (−11.55)	−491.270261	0.00	70.38	0.00	−11.37 (−10.69)
U1−2	−491.236276	+1.20 (+1.71)	70.63	+1.21	−13.31 (−9.84)	−491.267428	+1.77 (+1.78)	70.30	+1.69	−9.60 (−8.91)
U1−3	−491.235035	+1.98 (+2.59)	70.66	+2.02	−12.53 (−8.96)	−491.266334	+2.46 (+2.48)	70.16	+2.24	−8.91 (−8.21)
U1−4	−491.231015	+4.50 (+5.12)	70.43	+4.31	−10.00 (−6.43)	−491.263262	+4.39 (+4.37)	70.01	+4.02	−7.00 (−6.32)
uracil + $2H_2O$										
U2−1	−567.671655	0.00	86.73	0.00		−567.713331	0.00	86.35	0.00	
U2−2	−567.667218	+2.78	86.53	+2.58		−567.708794	+2.84	86.19	+2.68	
U2−3	−567.666058	+3.51	86.33	+3.11		−567.706857	+4.06	85.95	+3.66	
U2−4	−567.663143	+5.34	86.11	+4.72		−567.705140	+5.14	85.82	+4.61	
U2−5	−567.658355	+8.34	86.13	+7.74		−567.699465	+8.70	85.61	+7.96	
uracil + $3H_2O$										
U3−1	−644.099762	0.00				−644.150288	0.00	101.93	0.00	
U3−2	−644.096374	+2.13				−644.147779	+1.57	101.76	+1.40	
U3−3	−644.094206	+3.49				−644.145755	+2.84	101.80	+2.72	
U3−3′	−644.092980	+4.26				−644.145203	+3.19	101.55	+2.81	
uracil + $4H_2O$										
U4−1	−720.531515	0.00				−720.591101	0.00	117.74	0.00	
U4−2	−720.515762	+9.88				−720.578192	+8.46			
uracil + $7H_2O$										
U7−1						−949.895489	0.00	164.12	0.00	
U7−1′						−949.893648	+1.15	163.99	+1.03	

[a] In parentheses are reported the energy values estimated by taking into account the BSSE correction. [b] E_e (in a.u.) and E_v (in kcal/mol) represent the electronic and zero-point vibrational (ZPVE) energies, respectively. [c] $E_t = E_e + E_v$. E_t (in a.u.) is the total energy of the molecular compound. [d] E_d (in kcal/mol) is the binding energy of uracil + $1H_2O$.

TABLE 2: Geometrical Parameters of Isolated Uracil, Isolated Water, and Water Dimer[a]

bond lengths	calc.[b] 6-31G*	calc.[b] 6-31++G*	exp.[c]	bond angles	calc.[b] 6-31G*	calc.[b] 6-31++G*	exp.[c]
Uracil							
N1−H1	1.010	1.012	0.836 (1.002)	C2−N1−C6	123.7	123.6	122.7 (123.2)
N1−C2	1.396	1.394	1.371 (1.399)	C6−N1−H1	121.4	121.2	112.1 (121)
C2═O2	1.217	1.220	1.215 (1.212)	H1−N1−C2	114.8	115.1	115.1 (115.1)
C2−N3	1.385	1.385	1.377 (1.399)	N1−C2═O2	122.7	122.6	123.7 (123.8)
N3−H3	1.014	1.015	0.877 (1.002)	N1−C2−N3	112.7	113.1	114.0 (114)
N3−C4	1.414	1.412	1.371 (1.399)	O2═C2−N3	124.5	124.2	122.3 (121.9)
C4═O4	1.219	1.233	1.245 (1.212)	C2−N3−H3	115.5	115.6	117.8 (129.3)
C4−C5	1.460	1.460	1.430 (1.462)	C2−N3−C4	128.3	127.9	126.7 (126)
C5−H5	1.081	1.082	0.970 (1.072)	H3−N3−C4	116.1	116.3	115.5 (116.1)
C5═C6	1.350	1.352	1.340 (1.343)	N3−C4═O4	120.3	120.1	119.2 (120.2)
C6−H6	1.085	1.085	0.957 (1.072)	N3−C4−C5	113.3	113.6	115.5 (115.5)
C6−N1	1.375	1.377	1.359 (1.399)	O4═C4−C5	126.2	126.1	125.3 (124.3)
				C4−C5−H5	118.1	118.2	118.1 (118.9)
				C4−C5═C6	119.9	119.8	118.9 (119.7)
				H−C5═C6	121.9	121.9	123.0 (122.5)
				C5═C6−H6	122.8	122.8	123.2 (122.8)
				C5═C6−N1	121.9	121.8	122.3 (122.1)
				H6−C6−N1	115.2	115.3	114.5 (115.1)
Water							
O−H	0.969	0.969	0.957	H−O−H	103.8	105.5	104.5
Water Dimer[d]							
O−H (W1)	0.977	0.977		H−O−H′(W1)	104.1	105.9	
O−H′ (W1)	0.968	0.969					
O−H (W2)	0.970	0.970		H−O−H′(W2)	104.1	105.7	
O−H′ (W2)	0.970	0.970					
O(W1)···O(W2)	2.862	2.870	2.946	O−H(W1)···O(W2)	165.8	171.0	

[a] Bond lengths and angles are in angstroms and degrees, respectively. [b] Calc. Calculated values at the DFT/B3LYP level. The optimized geometries obtained at the B3LYP/6-31++G* level are displayed in Figure 1. [c] Exp. Observed values from X-ray data of uracil (ref 38). In parentheses are reported the observed values obtained from electron diffraction data (ref 39). The observed values for water and water dimers are from refs 43 and 41, respectively. [d] The water molecules involved in water dimer are labeled W1 and W2 (Figure 1).

conclusion by geometry optimization with two starting points corresponding to a linear and a cyclic water dimer without any structural constraint. We have found that the geometry optimization on both initial configurations leads to a unique linear water dimer (Figure 1). The use of 6-31++G* (versus 6-31G*) basis set leads to a more linear water dimer (Table 2). In fact, the O−H(W1)···O(W2) hydrogen bond angle varies from 165.8° (6-31G* basis set) to 171.0° (6-31++G* basis set).

Without BSSE correction, the water dimer binding energy (E_d) depends strongly on the basis set used. In fact, this energy increases by ∼1.4 kcal/mol in going from 6-31G* to 6-31++G* basis set (Table 1). BSSE correction affects (i) the absolute value

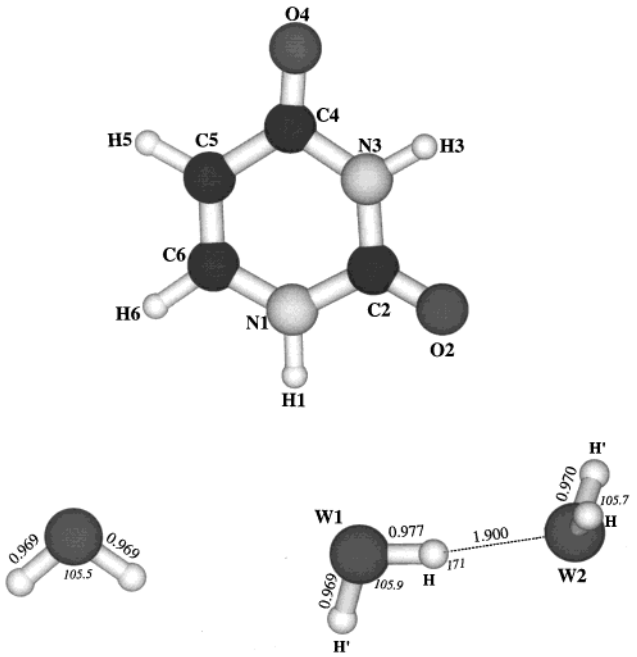

Figure 1. Graphical representation of optimized geometries of isolated uracil, isolated water, and water dimer obtained at the B3LYP/6-31++G* level. Bond lengths and H-bond distances (Å) are reported in bold, and valence angles and H-bond angles (degrees) are indicated in italic.

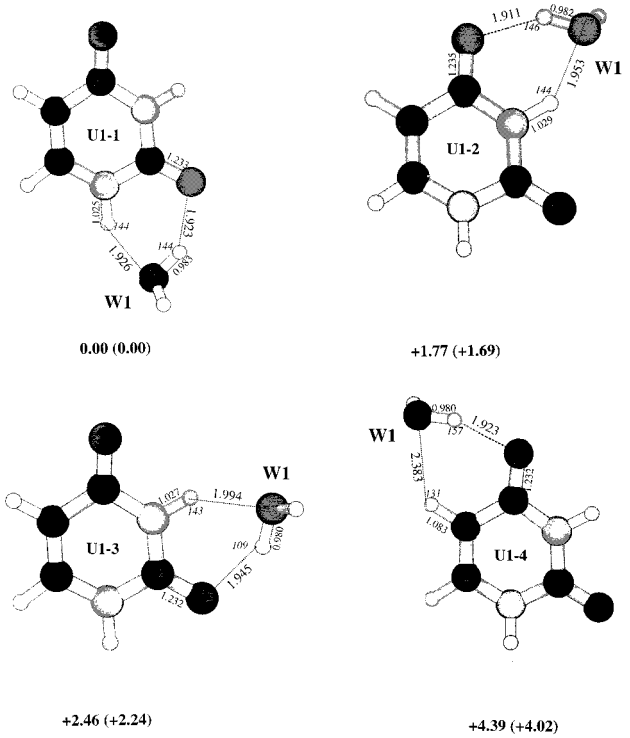

Figure 2. Graphical representation of uracil + $1H_2O$ optimized geometries obtained at the B3LYP/6-31++G* level. See the text for notations and Table 1 for the energy data of different configurations. See also the caption of Figure 1. ΔE_e and ΔE_t (in parentheses) values are noted below each configuration.

of the binding energy for a given basis set and (ii) the difference between the binding energies calculated with each of the basis sets used. It is worth mentioning that both water dimer BSSE corrected E_d values are very close to the experimental value (-5.4 ± 0.7 kcal/mol).[43]

Uracil + $1H_2O$. Four different configurations of this complex have been taken into consideration and labeled as U1−1, U1−2, U1−3, and U1−4 in an increasing order of their energy (Table 1, See Figure 2 for their graphical representation).

As it can be seen, the water molecule participates in each case in the formation of two hydrogen bonds with two adjacent sites of uracil, i.e., H1 and O2 in U1−1, H3 and O4 in U1−2, H3 and O2 in U1−3, and finally O4 and H5 in U1−4. These four configurations are located within a 4.0 to 4.5 kcal/mol energy range, and their energy order is the same whether obtained by means of ΔE_e or ΔE_t (Table 1). We stress the existence of a weak C5−H···O(W1) hydrogen bond in U1−4, which replaces a strong N−H···O(W1) hydrogen bond in the other configurations. This explains the higher energy of the U1−4 configuration compared to the other configurations. All or part of these four configurations have been treated in previous calculations at the HF,[17] MP2,[18,19] DFT,[20] and MBPT[22] levels. The common point between the former and the present calculations is the energy order of these configurations. However, at the MP2 and MBPT levels,[18,22] the energy difference between U1−1 and U1−4 does not exceed 3.50 kcal/mol.

BSSE correction does not affect the energy order of uracil + $1H_2O$ configurations (Table 1), regardless of the basis set used. However, it leads to an increase of their E_d values. We emphasize here the joint effects of BSSE correction and the basis set used. In fact the initial and corrected E_d values differ by 3.0 to 3.5 kcal/mol upon the use of 6-31G* basis set, and only by 0.7 kcal/mol in the case of the 6-31++G* basis set. Thus, the difference between electronic energies of these conformers is altered considerably (by 0.5 to 0.6 kcal/mol) when BSSE corrections are done with 6-31G* basis set, whereas ΔE_e values remain unchanged (altered only by 0.01 to 0.02 kcal/mol) upon BSSE corrections with the 6-31++G* basis set. It seems reasonable to claim here that BSSE corrections have no effect on the energy order of configurations when the basis set is enriched with diffuse orbitals (for instance, the 6-31++G* basis set). At last, the present E_d values in uracil + $1H_2O$ configurations, with or without BSSE corrections, are in good agreement with previous calculations performed at different theoretical levels.[18−22]

From the geometrical point of view, one can first mention a lengthening of about 0.012 Å in both N1−H (in U1−1) and N3−H (in U1−2 and U1−3) bonds upon complexation with water molecule. The lengthening behavior of carbonyl bonds depends on their location on uracil ring: C2═O2 bond length is increased by 0.013 Å (in U1−1 and U1−3), whereas C4═O4 bond length remains unaltered in U1−2 and U1−4 upon hydrogen bonding. This invariance is also true in the case of a C5−H bond involved in a hydrogen bond with a water molecule (U1−4). The O−H bond of the water molecule involved in an intermolecular H-bond with uracil, is always increased by about 0.012 Å, whereas the free O−H maintains its initial value (0.969 Å), as in the water monomer (Table 1). On the other hand, the average value of the N−H···O(W1) hydrogen bond distances (1.958 Å) is longer than those of C═O···H(W1) type (1.926 Å) (Figure 2). The C−H···O(W1) hydrogen bond distance is the longest one (2.383 Å, see U1−4 in Figure 2) among all of the intermolecular H-bonds evidenced by the present calculations. At last, we can mention that uracil keeps globally its planar geometry upon complexation with a water molecule, and in all configurations the free hydrogen of water (not involved in H-bond) is perpendicular to the uracil plane.

Uracil + $2H_2O$. Five different configurations are optimized and labeled as U2−1, ..., U2−5 (Figure 3). As in the case of the uracil + $1H_2O$ complex, the effect of both basis sets has been analyzed on electronic and vibrational energies of this

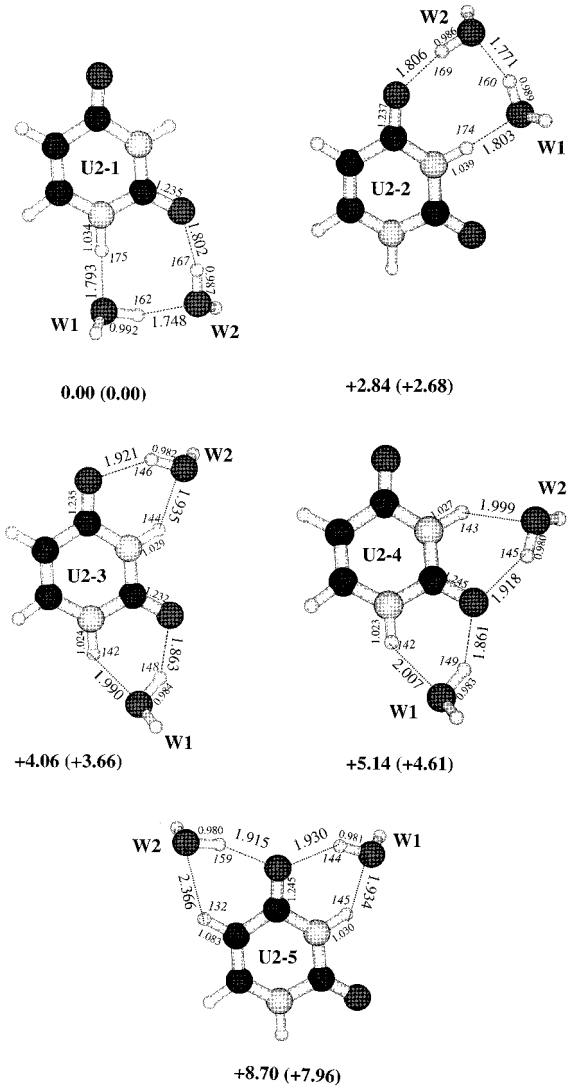

Figure 3. Graphical representation of uracil + $2H_2O$ optimized geometries obtained at the B3LYP/6-31++G* level. See the text for notations and Table 1 for the energy data of different configurations. See also the captions of Figures 1 and 2.

complex (Table 1). Although the vibrational energies seem to be independent of the basis set used, a general increase in total energy differences (ΔE_t) is to be emphasized upon the use of the 6-31++G* basis set. The two lowest energy configurations, i.e., U2−1 and U2−2, correspond to the uracil−water complexation with a water dimer hydrogen bonded to H1 and O2 on one hand (U2−1), and to H3 and O4 on the other hand (U2−2). This result is in concordance with those obtained on the uracil + $1H_2O$ complex, where the two lowest energy configurations (U1−1 and U1−2, Figure 2) include hydrogen bonds on the same sites of uracil molecule. It should be mentioned that U2−1 and U2−2 configurations as displayed here with the mutual orientations of hydrogens (either involved in H-bonds or not) represent the lowest energy configurations. All of our attempts to select other orientations of water molecule hydrogen atoms in order to keep the same number of intermolecular H-bonds led to higher energy configurations.

The U2−3 configuration, which is energetically located just above the two previous ones (Table 1), contains intermolecular H-bonds with a water monomer located on each of the above-mentioned molecular sites. The molecular energy continues to increase when two water monomers are hydrogen bonded with three adjacent donor−acceptor sites of uracil, i.e., H1, O2, H3 in U2−4 and H3, O4, H5 in U2−5. As in the case of the uracil + $1H_2O$ complex, the highest energy configuration of uracil + $2H_2O$ is that including a C5−H···O(W) hydrogen bond (U2−5, Figure 2).

One of the most interesting effects evidenced upon the comparison of the lowest energy configurations of uracil + $2H_2O$ (U2−1 and U2−2, Figure 3) with those of uracil + $1H_2O$ (U1−1 and U1−2, Figure 2) is the considerable shortening of N−H···O(W) and C═O···H(W) hydrogen bonds (by 0.10 to 0.15 Å) when a water monomer is replaced by a water dimer. This fact is also valid for the H-bond distance of the water dimer bound to uracil (Figures 1 and 3). Another effect that is worth of mentioning is that the N−H···O(W) and C═O···H(W) hydrogen bonds displayed in U2−1 and U2−2 become *linear* in comparison with those in U1−1 and U1−2 configurations. In contrast, the linearity of the O−H(W1)···O(W2) hydrogen bond is comparatively decreased in going from a free water dimer to that bound to uracil (Figures 1 and 3). Moreover, U2−3 cannot be considered as a simple superposition of U1−1 and U1−2, because N−H···O(W) and C═O···H(W) formed with water (W1) are altered considerably by the presence of the second water molecule (W2), and vice versa (Figures 2 and 3). At last, the lengthening of N−H and C═O bonds in U2−1 and U2−2 configurations is more pronounced than that encountered in U1−1 and U1−2. This is also the case for the O−H bond lengths of water molecules involved in hydrogen bonds, either with each other or with uracil. It should also be noticed that there is a notable increase in C2═O2 and C4═O4 bond lengths in U2−4 and U2−5, respectively, upon complexation with two water monomers on each side of O2 (U2−4) and O4 (U2−5) (see for details the comparison between U1−1 and U2−4 on one hand, and between U1−2 and U2−5 on the other hand, in Figures 2 and 3).

Uracil + $3H_2O$. The energy data of the four configurations analyzed in this step, labeled as U3−1, U3−2, U3−3, and U3−3′, are reported in Table 1 (See Figure 4 for their graphical representation.) In these configurations, the three water molecules are bound to uracil as a water dimer and a water monomer (U3−1 and U3−2), or as a water trimer (U3−3 and U3−3′). On the basis of the results for uracil + $1H_2O$ (Figure 2) and uracil + $2H_2O$ (Figure 3), it is not surprising that U3−1 and U3−2 correspond to the lowest energy configurations, because (i) they both involve a water dimer, and (ii) all intermolecular H-bonds are formed with the most energetically favorable donor and acceptor sites of uracil. Moreover, the hydrogen bond patterns formed in U3−1 cannot be considered as a simple superposition of those appearing in U1−2 (Figure 2) and U2−1 (Figure 3) configurations. This is also valid when U3−2 (Figure 4) is compared with U1−3 (Figure 2) and U2−1 (Figure 3) configurations. In fact, subtle differences appear in the hydrogen bond distances between uracil and W3 water molecule. In the U3−1 conformation, C4═O4···H(W3) is lengthened by 0.046 Å and N3−H3···O(W3) is shortened by 0.047 Å, when compared to those appearing in U1−2. In U3−2, the N3−H3···O(W3) distance is not affected, whereas the C2═O2···H(W3) distance is shortened by 0.011 Å, when compared to those in U1−3.

To optimize other energetically significant configurations of uracil + $3H_2O$, we selected in a further step two of them as labeled U3−3 and U3−3′. The reasons behind this fact are as follows. (i) Both of these configurations contain a water trimer (which leads to a notable decrease of supermolecular energy) in front of O2 and H1 atoms (Figure 4), i.e., the most favorable uracil sites for hydrogen bond formation (see the results for

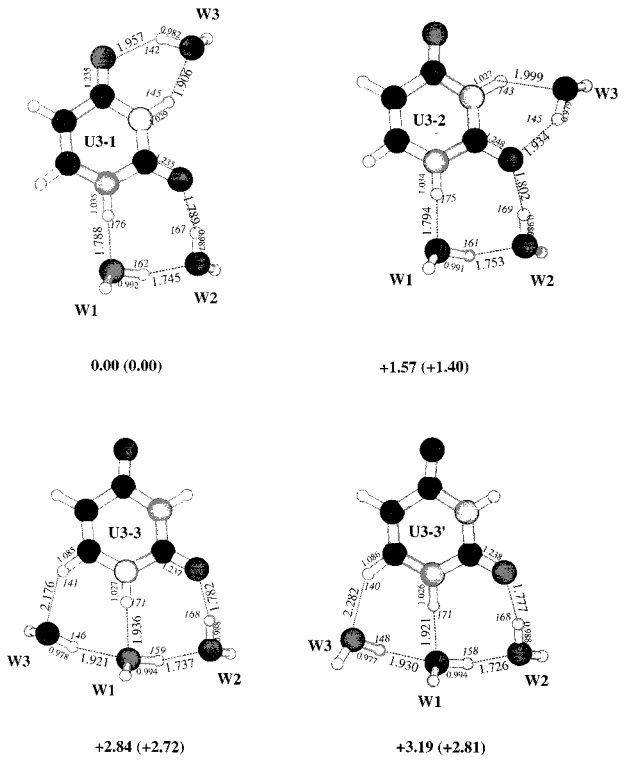

Figure 4. Graphical representation of uracil + $3H_2O$ optimized geometries obtained at the B3LYP/6-31++G* level. See the text for notations, and Table 1 for the energy data of different configurations. See also the captions of Figures 1 and 2.

uracil + $1H_2O$ and uracil + $2H_2O$). (ii) All of our attempts to optimize a configuration with a water trimer simultaneously H-bonded to O2, H3, and O4 sites of uracil, were unsuccessful (either at 6-31G* or 6-31++G* basis set). (iii) All other possibilities to form hydrogen bonds between a water trimer and uracil would contain one or two less favorable C−H···O(W) interactions. The presence of the weak C6−H···O(W3) hydrogen bond in U3−3 and U3−3′ configurations explains their energy increase with respect to the lowest energy ones, despite the energy decrease implied by the presence of a water trimer. Geometrically, the main difference between U3−3 and U3−3′ configurations is the orientation of the free hydrogen of W3 water molecule with respect to the uracil plane. As reported in Table 1, the electronic energy of U3−3 and U3−3′ configurations differs by 0.35 kcal/mol (see results obtained at the B3LYP/6-31++G* level), whereas upon the addition of ZPVE, their total energy is separated by only 0.09 kcal/mol. This means that U3−3 and U3−3′ correspond to two approximately degenerate configurations of uracil + $3H_2O$ complex.

A direct consequence of water trimerization between H6 and O2 sites of uracil is mainly the strong lengthening (> 0.13 Å) of the N1−H1···O(W1) hydrogen bond in going from U2−1 (Figure 3) to U3−3 and U3−3′ (Figure 4) configurations. Moreover, the O−H(W1)···O(W2) H-bond distance is decreased in going from U2−1 to U3−3 or U3−3′ by 0.011 and 0.022 Å, respectively. On the other hand, the O−H(W3)···O(W1) H-bond distance is longer than that obtained in the isolated water dimer (increased by 0.030 Å).

Uracil + $4H_2O$. As it can be concluded from the preceding paragraphs, the number of possiblities to form energetically favorable uracil + n_wH_2O configurations decreases when n_w increases. However, by keeping in mind the results obtained for $n_w < 4$, we have selected in this step two configurations

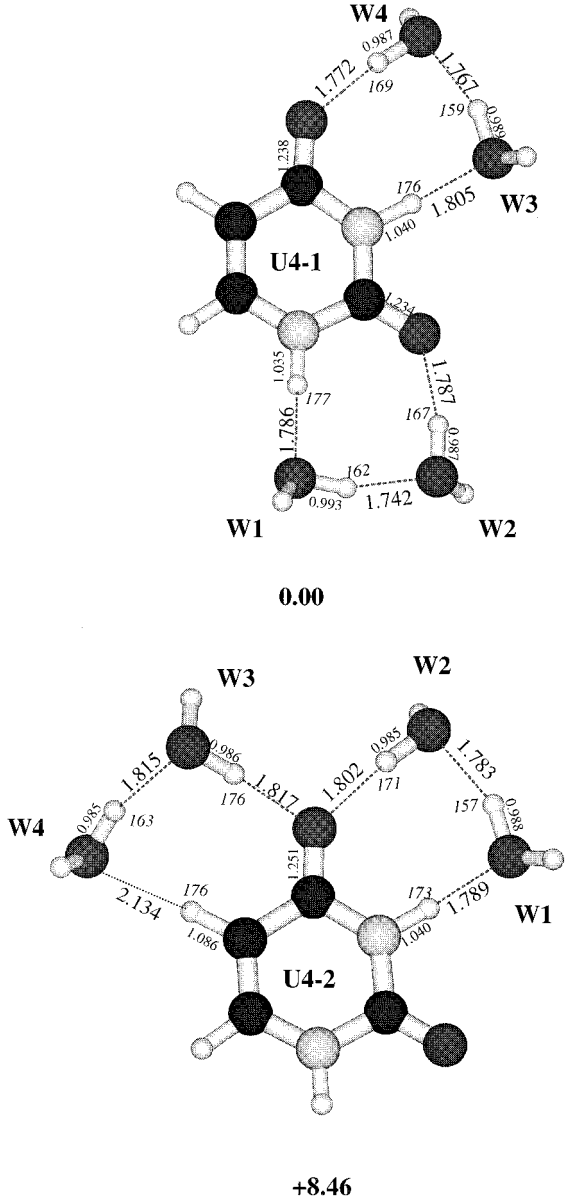

Figure 5. Graphical representation of uracil + $4H_2O$ optimized geometries obtained at the B3LYP/6-31++G* level. See the text for notations, and Table 1 for the energy data of different configurations. See also the captions of Figures 1 and 2.

labeled as U4−1 and U4−2, whose usefulness to achieve the first hydration shell will be detailed later. See Table 1 for the energy data of these configurations and Figure 5 for their graphical representation. The lowest energy configuration (U4−1) is a combination (and not a simple superposition as previously observed) of the lowest energy configurations of uracil + $2H_2O$ (U2−1 and U2−2, Figure 3). Correspondingly, the U4−2 configuration is a logical extension of the U2−5 configuration (Figure 3) with two water dimers (replacing two water monomers) at each side of the uracil O4 site.

The main new geometrical result obtained here is that, in contrast to all other configurations obtained up to now, U4−2 present intermolecular hydrogen bonds, i.e., C4═O4···H(W2) and C4═O4···H(W3), formed on each side of uracil plane.

Uracil + $7H_2O$. On the basis of all the above-mentioned results on uracil + n_wH_2O (n_w = 1, ..., 4), we have shown how the donor and acceptor sites of uracil can be surrounded by either water monomers, water dimers, or water trimers. The aim of this paragraph is to describe how to combine all of these results

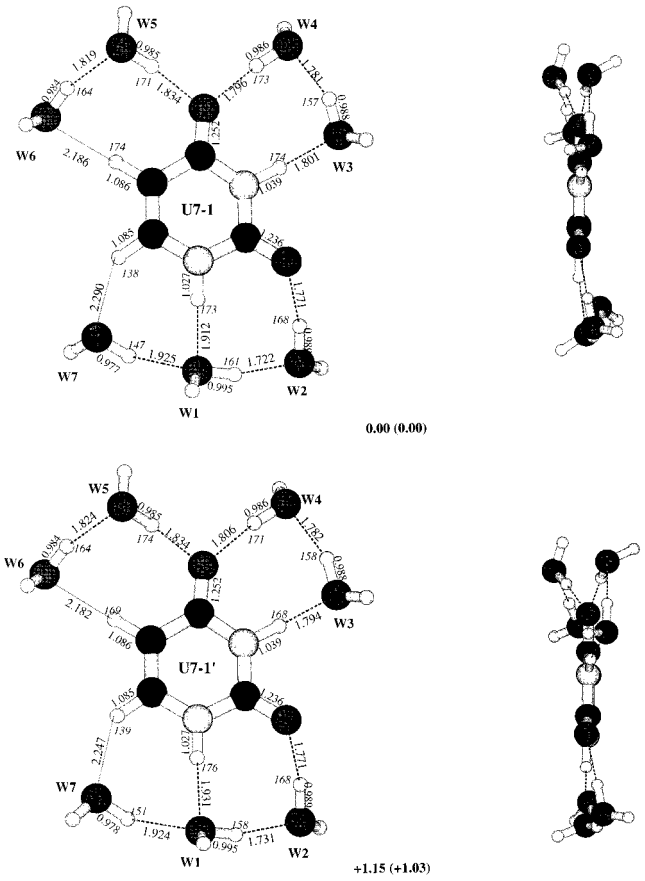

Figure 6. Graphical representation of uracil + $7H_2O$ optimized geometries obtained at the B3LYP/6-31++G* level. Left: hydrated uracil with a perpendicular view to the base plane. Right: hydrated uracil with a parallel view to the base plane. See the text for notations, and Table 1 for the energy data of different configurations. See also the captions of Figures 1 and 2.

in order to (i) achieve the closure of the first hydration shell in an average plane containing uracil, (ii) obtain the most energetically favorable configuration corresponding to the first hydration shell. To reach this objective, we have been inspired from our results concerning uracil + $3H_2O$ and uracil + $4H_2O$, especially those that allow us to cover all donor and acceptor sites of uracil. In our selection, we have also taken into account those configurations including water dimers or water trimers that particularly led to a considerable energy decrease of water−water interactions. As it can be seen in Figures 4 and 5, the most suitable configurations that can be combined together are the U3−3 (or U3−3′) and U4−2 configurations, giving rise to two different configurations labeled U7−1 and U7−1′. The results of the optimized geometries for uracil + $7H_2O$ obtained at the B3LYP/6-31++G* level are displayed in Figure 6. Table 1 provides the energy data of these configurations and shows that although U3−3 and U3−3′ correspond to two degenerate states (as mentioned above), U7−1 and U7−1′ do not follow the same trend: their total energies are separated by 1.03 kcal/mol.

III.2. Vibrational Features. In this section our attention will be focused particularly on the main vibrational modes of uracil in going from isolated to hydrated states.

Isolated Uracil, Isolated Water, and Water Dimer. The reliability of the calculated vibrational modes of uracil, isolated water, and water dimer can be verified on the basis of the observed values in gas phase[44] or in matrix isolated spectra.[45−47] This comparison has been made in Table 3 by mentioning both the theoretical vibrational wavenumbers at the B3LYP/6-31G* and B3LYP/6-31++G* levels, for these molecular compounds. As it can be easily verified (Table 3), the calculated wavenumbers for isolated water and water dimer at the B3LYP/6-31++G* are generally closer to the observed wavenumbers. In fact, although the O−H bond stretch vibrations are not sensitive to the choice of basis set, the H−O−H scissoring wavenumber undergoes a large downshift (∼50 cm^{-1}) upon the use of diffuse orbitals, getting closer to the observed values.

In a recent work devoted to neutron inelastic scattering (NIS) spectra of nucleic acid constituents,[33] we have reported and discussed the full assignment of the isolated uracil vibrational modes and its deuterated species calculated at the B3LYP/6-31G* level. In Table 3 are reported the wavenumbers calculated with both 6-31G* and 6-31++G* basis sets, and compared with those observed in gas phase and Ar matrix. One can state that the wavenumber values located above 1500 cm^{-1} are undoubtedly improved upon the use of diffuse orbitals, whereas in the region below 1500 cm^{-1}, the wavenumbers are not considerably affected by one or the other basis sets.

At the B3LYP/6-31++G* level, the O−H symmetric bond stretch of isolated water, is downshifted by 100 cm^{-1} upon the hydrogen bonding between water molecule (see results for W1 in water monomer and water dimer in Table 3). In contrast, upon H-bonding, the O−H asymmetric bond stretch is downshifted by only 30 cm^{-1}. The two H−O−H scissoring wavenumbers calculated in water dimer show ∼30 cm^{-1} and ∼15 cm^{-1} upshift, compared to that corresponding to a water monomer. The interaction between the two water molecules provides six calculated vibrational modes located below 720 cm^{-1}. Unfortunately, no comparison with observed values can be done in this spectral range. However, the effect of the basis set on their values should be stressed, particularly for the lowest calculated wavenumber, which is upshifted by 140 cm^{-1} upon the use of diffuse orbitals.

Hydrated Uracil. It is a matter of fact that all of the intermediate supermolecules involving uracil and one to four water molecules (Figures 2−5) give partial and interesting information on the effect of uracil hydration on the vibrational modes. However, the analysis of all of the vibrational modes obtained from all of the optimized configurations (17 in total) is out of the scope of this paper. In this section, we limit our discussion to the vibrational modes calculated in the lowest energy configuration of the uracil + $7H_2O$ complex, i.e., U7−1 (Table 1, Figure 6).

Although, uracil + $7H_2O$ is not a model to treat all of the vibrational features of a completely hydrated uracil, it can provide a wealth of information on this subject, because all of the main donor and acceptor sites of the nucleic acid base are involved in the H-bond network with surrounding water molecules. On the basis of the calculated results, the coupling between the base and water molecule vibrational motions through intermolecular H-bonding can be verified in several spectral regions.

The vibrational modes calculated for the U7−1 configuration (Figure 6, Table 1) at the B3LYP/6-31++G* level, are reported in Table 4 and compared with IR and Raman spectra observed in aqueous solutions in the spectral region below 2000 cm^{-1}.[27] Recently, we have reported the vibrational modes calculated for the same configuration (U7−1) at the B3LYP/6-31G* level of theory.[48] The comparison between these two sets of results shows that the use of the diffuse functions improve considerably the wavenumbers associated with the vibrational motions of the chemical groups involved in the H-bond network with water molecules (e.g., C═O, N−H).

TABLE 3: Comparison between the Observed and Calculated Vibrational Wavenumbers of Uracil, Water Monomer, and Water Dimer

uracil					water monomer					water dimer				
obs.[a]	obs.[b]	calc.[c]	calc.[d]	assignments	obs.[e]	obs.[f]	calc.[c]	calc.[d]	assignments	obs.[e]	obs.[f]	calc.[c]	calc.[d]	assignments[g]
3485	3450	3641	3634	ν(N1−H)	3725	3734	3846	3847	ν(O−H) asymm.	3714	3724	3830	3842	ν(O−H) asymm. W2
3435	3427	3605	3594	ν(N3−H)	3632	3638	3722	3721	ν(O−H) symm.	3698	3710	3807	3812	ν(O−H) asymm. W1
3084	3101	3271	3267	ν(C5−H)						3626	3634	3715	3723	ν(O−H) symm. W2
	3076	3230	3230	ν(C6−H)						3574	3638	3618	3618	ν(O−H) symm. W1
1764	1734	1848	1810	ν(C2═O2)										
	1688	1811	1776	ν(C4═O4)										
1643	1632	1693	1680	ν(C5═C6); δ(C6−H)	1597	1589	1711	1662	δ(HOH)	1618	1611	1742	1692	δ(HOH) W2; W1
1472	1480	1513	1510	ν(N1−C6); δ(N1−H)						1600	1594	1707	1676	δ(HOH) W1; W2
1399	1396	1431	1430	δ(C6−H); δ(N3−H)										
1389	1380	1415	1417	δ(N−H)										
1360		1391	1393	δ(N3−H); ν(N−C)										
	1228	1239	1241	δ(C5−H); ν(N1−C6)										
1184		1204	1207	ν(N−C); δ(C6−H)										
1073	1089	1096	1095	ν(N1−C6); δ(C5−H)										
982	999	992	991	δ(ring)										
958	974	970	972	ν(ring)										
842	841	969	969	ω(C6−H); τ(C═C)										
804	810	817	816	ω(C5−H); ω(C4═O4)										
		773	772	ring-breathing mode										
759	769	758	747	ω(C2═O2)										
718		732	726	ω(C4═O4); ω(C6−H)										
662	672	691	686	ω(N3−H); τ(C−N)								705	717	W1−W2
559	588	563	568	ω(N1−H); τ(N−C)										
551	556	558	558	δ(C2═O2); δ(ring)										
536	527	541	541	δ(C═O); δ(ring)										
516		519	521	δ(ring)								462	417	W1−W2
391	411	395	397	ω(N1−H); ω(C5−H)										
	377	385	385	δ(C═O)								234	226	W1−W2
	185	170	168	τ(ring); ω(N1H)								179	195	W1−W2
		149	150	ω(N3H); τ(ring)								152	176	W1−W2
												22	162	W1−W2

[a] Observed IR spectra of uracil in Ar matrix (ref 45). [b] Observed IR spectra of uracil in gas phase (ref 44). [c] Calculated at the B3LYP/6-31G* level. [d] Calculated at the B3LYP/6-31++G* level. [e] Observed IR spectra in N2-matrix at T = 20 K (ref 46). [f] Observed IR spectra in Ar matrix at T = 7 K (ref 47). [g] W1 and W2 denote the two water molecules involved in a water dimer (Figure 1). W1−W2 means that the vibrational mode arises from the interaction between the two water molecules in the dimer. Notations: ν (bond-stretch), δ (angle deformation), ω (out-of-plane wagging), and τ (torsion mode).

The calculated vibrational modes of water molecules have no counterpart in the observed spectra, owing to the buffer subtraction performed in the experimental analysis of hydrated uracil. The effect of water dimerization and trimerization and their interaction with uracil can, however, be detected on the O−H bond stretchings, through the comparison of the wavenumbers of water molecules interacting with uracil (Table 4) and those calculated for water dimer (Table 3).

As far as the uracil vibrational modes are concerned, N−H bond stretch vibrations are considerably downshifted (∼300 to 400 cm^{-1}), whereas its C−H bond stretch vibrations are less affected (∼30 cm^{-1}) upon interaction with surrounding water molecules. C═O bond stretches are downshifted and their assignments clearly show the participation of water molecules in these vibrations. Other uracil in-plane vibration modes located in the region between 1670 and 1000 cm^{-1} are also affected by the presence of water molecules. Calculated wavenumbers are generally located above the observed wavenumbers.

Below 1000 cm^{-1}, the agreement between theoretical and observed wavenumbers for in-plane modes is improved considerably. The ring breathing mode of uracil observed in the Raman spectrum is very well assigned (calc. 798 cm^{-1}, obs. 782 cm^{-1}). Other in-plane modes, all observed in Raman spectrum between 580 and 480 cm^{-1}, are also well assigned by vibrational calculations.

The most interesting point is the effect of hydration on the out-of-plane wagging modes of N−H, C−H, and C═O groups of uracil. First of all, N1−H and N3−H waggings are considerably upshifted from 568 and 686 cm^{-1} (calculated in isolated uracil, Table 3) to 985 and 973 cm^{-1} (Table 4), respectively. To a lesser extent, the C−H wagging wavenumbers are also altered. Note the wavenumber upshift of C5−H from 816 to 904 cm^{-1} (Tables 3 and 4) owing to the interaction with W5−W6 water dimer (Figure 6). In contrast, C6−H wagging is downshifted from 969 to 891 cm^{-1} upon the interaction with W7−W1−W2 water trimer (Figure 6). The smallest wavenumber upshifts (20 to 30 cm^{-1}) concern the C═O wagging modes (Tables 3 and 4).

IV. Concluding Remarks

Water is a highly polar molecule which can simultaneously play the role of an H-bond acceptor and donor via the interactions occurring through its oxygen or hydrogen atoms, respectively. H-bonding can also occur between water molecules either in the bulk or in the vicinity of a host molecule, thus leading to a notable decrease of the overall supermolecular energy.

In this paper, we have reported at the DFT level of theory a systematic search to find the most suitable interaction sites of uracil with surrounding water molecules. The energy order of different uracil + $n_w H_2O$ configurations relative to a given number n_w of water molecules has been calculated and discussed in the text.

Although these calculations concern an isolated base and not that involved in nucleic acid, which is generally connected through the N1 atom to a sugar residue, the results obtained here allow us to scan the ability of the different molecular sites

TABLE 4: Comparison between the Calculated (in U7−1 Configuration) and Observed (in aqueous phase) Vibrational Wavenumbers of Uracil

obs.[a]	obs.[b]	calc.[c]	assignments[d]	obs.[a]	obs.[b]	calc.[c]	assignments[d]
		3825	ν(O−H) asymm. W7			753	ω(C═O); W2−U; W4−U
		3814	ν(O−H) asymm. W5			745	ω(C═O); W6−U; W5−U
		3812	ν(O−H) asymm. W3			691	W5−U; W5−W6
		3810	ν(O−H) asymm. W2			657	W1−W7; W1−W2
		3808	ν(O−H) asymm. W6	573		584	δ(C═O); W1−U
		3805	ν(O−H) asymm. W4	553		579	δ(C4═O); W6−U; δ(ring); W5−U
		3790	ν(O−H) asymm. W1	536		551	δ(ring); W3−U; δ(C5−H)
		3633	ν(O−H) symm. W7			486	W1−W7; W1−W2; W3−W4; ω(N3−H)
		3536	ν(O−H) symm. W5, W6			483	W3−W4; W5−W6; δ(C═O)
		3501	ν(O−H) symm. W3, W4, W6	423		452	W5−W6; W5−U; δ(C5−H)
		3479	ν(O−H) symm. W3, W4, W5, W6	401		439	ω(N1−H); ω(C5−H); W7−U; τ(C═C)
		3453	ν(O−H) symm. W2			431	W5−W6; W2−U
		3419	ν(O−H) symm. W3, W4			424	W5−W6; W5−U; W2−U; W6−U; δ(C2═O)
		3375	ν(N1−H); ν(O−H) symm. W1			401	W4−U; W5−W6
		3285	ν(O−H) symm. W1; ν(N1−H)			387	W5−W6; W5−U; δ(C═O)
		3239	ν(C6−H)			375	W1−U; W5−W6; W1−W7
		3204	ν(C5−H); W6−U			355	W1−U; W1−W7; ω(N1−H)
		3178	ν(N3−H)			315	W3−U; W3−W4; ω(N3−H)
1708	1710	1778	ν(C2═O); W3−U			305	W1−W2; W1−W7
		1735	δ(HOH) W1, W2			279	W3−U; W3−W4; ω(N3−H)
		1731	δ(HOH) W1, W4, W5, W6			260	W1−W2; W1−W7
		1716	δ(HOH) W4, W5, W6			256	W3−U; W3−W4; ω(N3−H)
1677	1675	1709	δ(HOH) W2,W4; δ(C5−H); ν (C4═O)			250	W5−W6; W5−U; W6−U; δ(C═O)
		1706	δ(HOH) W1, W2, W4			239	W5−W6; W5−U; W6−U; ω(C5−H)
		1697	δ(HOH) W3, W5, W6			218	W5−U; W2−U; W3−U; W5−W6
		1687	δ(HOH) W3, W5; δ(C5−H)			200	W3−U; W4−U; W6−U; τ(C−N)
		1672	δ(HOH) W7			195	W6−U; τ(ring); W2−U; ω(N−H); τ(C−C)
1637	1640	1663	ν(C═C); ν (C4═O); δ(C6−H)			188	W6−U; W5−U; W5−W6; W1−U; W4−U
1504	1506	1561	δ(N1−H); ν(C2═O); ν(N1−C6)			180	W6−U; W5−W6; W3−U; W3−W4; τ(C−N)
1449	1448	1513	W3−U; δ(N3−H); ν(C═O)			173	W1−W2; W1−W7; δ(C4═O)
1413	1414	1461	ν (C4═O); δ(C5−H);ν(ring);δ(ring)			154	W6−U; W5−W6; W5−U; W2−U
1387	1391	1438	δ(C−H); ν(C−N); ν(C═C)			147	W7−U; W5−W6; W5−U; δ(C4═O)
		1286	δ(C−H);ν(N1−C6);ν(C−C);W6−U			143	W5−W6; W6−U; W5−U; W7−U
1232	1222	1264	ν (ring); W6−U			135	W1−U; W1−W2
1091		1149	W6−U; δ(C−H); ν(N1−C6); ν(C═C)			113	W5−W6; W6−U; W5−U; δ(C5−H)
1001	1000	1037	W6−U; ω(C6−H); τ(C═C); τ(C−N)			105	W7−U; W5−W6
	993	1029	ν(C−C); δ(C5−H); W3−U, W6−U, W7−U			94	W1−U; W3−U; W5−W6; δ(N3−H)
966		1000	W3−U; δ (ring)			76	W6−U; W3−U; W4−U; τ(C−N)
		985	W1−W2; W2−U; ω(N1−H)			61	W5−W6; W1−U; W2−U; τ(C−N)
		973	W3−U; W6−U; ω(N3−H)			58	W1−U; W1−W7; W3−U
		943	W4−U; W3−W4; W3−U; δ(N3−H)			51	W6−U; W5−U; W2−U; W1−U
		904	W6−U;W5−W6;W1−U;ω(C5−H);ω(N1−H)			43	W6−U; W5−U; δ(C5−H)
		891	W6−U; W5−W6; ω(C6−H); ω(N1−H)			37	W6−U; W3−U; τ(C−N)
		843	W5−W6; W5−U			29	W5−U; W5−W6; ω(N−H)
782		798	ring breathing mode			25	W6−U; W2−U; W4−U; ω(C5−H)
		767	W2−U; W1−W2; ω(C2═O)			20	W4−U; τ(C═C)
		755	W4−U; ω(C4═O); W5−W6; W3−W4				

[a] Observed in Raman spectra of uracil in aqueous solution (ref 27). [b] Observed in IR spectra of uracil in aqueous solution (ref 27). [c] Calc. Calculated values at the DFT/B3LYP/6-31++G* level. [d] W1, ..., W7 designates the water molecules interacting with uracil. W1−W2, ..., etc. means the interaction between pair of water molecules, whereas W1−U, ...etc. designates the uracil−water interactions. See also the notations in Table 3.

to interact with surrounding water molecules. The interaction of the bigger size nucleic acid constituents, such as nucleosides and nucleotides with explicit water molecules, should now be considered at the quantum mechanical level.

As it has been shown above, seven water molecules are needed in order to achieve the closure of the first hydration shell in an average plane containing uracil. We have verified by several additional calculations that the introduction of more water molecules around uracil contributes preferentially to the formation of the second hydration shell (in the plane of uracil). In fact, the aim of this paper was to analyze the H-bonds that can be formed between uracil and those water molecules located in the first hydration shell (in the plane of uracil), rather than to focus on the three-dimensional H-bond network between water molecules.

In each step, vibrational calculations allowed us to assign the supermolecular configurations to energy minima, and to estimate more precisely the ground-state energy of these configurations by considering the calculated ZPVE for each of them. The energy order of different configurations corresponding to a given n_w value is independent of the basis sets used, i.e., 6-31G* and 6-31++G*. However, some subtle differences between the calculations performed with these two basis can be emphasized. For instance, for $n_w = 1-2$, ΔE_e values generally increase upon the use of diffuse orbitals, whereas they decrease for $n_w = 3$. The addition of ZPVE does not change the energy order, but it decreases the difference between total energies of different configurations corresponding to a given n_w value. Nevertheless, the use of the 6-31++G* basis set is necessary to improve both the geometrical and vibrational results. In particular, N−H···O(W) and C═O···H(W) intermolecular H-bond distances increase by 0.020 Å to 0.083 Å when diffuse orbitals are used, thus in better agreement with the known H-bonding patterns. Moreover, calcu-

lated wavenumbers at 6-31++G* are generally closer to the observed ones: a general downshift of wavenumber values is obtained.

Other conclusions derived from the present work can be summarized as follows. (a) In the case of uracil + $1H_2O$ configurations, the energy order found in this work corresponds exactly to that found in previous works.[18−22] Upon the use of diffuse orbitals, BSSE corrections can barely affect the energy differences separating various configurations of uracil+ $1H_2O$. However, a constant and small BSSE correction on the binding energies (0.7 kcal/mol) should be taken into consideration in all uracil + $1H_2O$ configurations. This is the reason our study of other uracil + n_wH_2O complexes ($n_w > 1$), for which we were only interested in the energy order of the optimized configurations, was carried out at the B3LYP/6-31++G* level without any BSSE corrections applied.

(b) The present results contradict somehow those previously published by other authors[25] claiming that the first hydration shell of uracil can be completed with only three water monomers hydrogen bonded to the base through H1 and O2(W1), O2 and H3(W2), O4 and H5(W3) sites. On the basis of all the present theoretical results obtained on uracil + n_wH_2O ($n_w = 1, 2, 3$), the above-mentioned configuration has a higher energy than U3−1, U3−2, and U3−3 (Figure 4) because in the previous calculations,[25] water dimer formation (leading to a notable energy decrease of the supermolecular system) was not considered, and the three water monomers are not simultaneously placed in the most favorable H-bonding sites of uracil.

(c) It should be mentioned that all uracil + n_wH_2O complexes display a planar geometry of uracil, as in the case of isolated uracil. One should also remark that the three C═O···H(W) (W2, W4, W5) intermolecular hydrogen bonds displayed in U7−1 (and in U7−1′) are systematically formed on one side or the other of the uracil plane (Figure 6), whereas N−H···O(W) and C−H···O(W) bonds are globally localized in the plane defined by uracil ring.

(d) We have verified that the uracil + $7H_2O$ configurations (described above, see Figure 6) present the maximum number of water molecules that the first hydration shell can accept in the plane of uracil. Two free zones where water molecules are absent should, however, be noticed, i.e., one between O2 and H3 and the other between H5 and H6. These two zones might be occupied by water molecules either located in the first hydration shell but out of the uracil plane, or by those belonging to a part of the second hydration shell.

The calculated vibrational modes issued from uracil + $7H_2O$ complex have been compared with those observed in aqueous solutions by means of Raman and IR spectroscopy. From this comparison, one can easily recognize the characteristic uracil vibrational motions in the list of the calculated modes. However, a strong coupling of these modes with water motions has been evidenced by the present calculations. Obviously, a routine scaling of the molecular force field obtained from isolated uracil could never reflect adequately its aqueous phase vibrational features. Thus, in the future, precise quantum mechanical calculations at molecular level in the presence of explicit water are necessary to interpret the observed vibrational spectra of nucleic acid constituents in aqueous phase. Our discussion of the uracil vibrational modes observed in aqueous phase by means of the calculated results from the uracil + $7H_2O$ complex clearly shows that a very good agreement has been obtained in the spectral region below 1000 cm^{-1}: the deviation between calculated and observed wavenumbers does not exceed 30 cm^{-1}. In the 2000−1000 cm^{-1} range, this deviation becomes larger (∼60 cm^{-1}). To alleviate the latter discrepancies, one can suggest to take into account other explicit water molecules located in the first hydration shell, but out of the uracil plane, and correct the vibrational calculations by considering anharmonic effects.

Finally it should be mentioned that a theoretical search, such as the present one or all other previous ones, yields a static picture of the base−water possible and energetically favorable interactions. A dynamic theoretical analysis of the uracil−water (or more generally nucleic acid base−water) at the quantum mechanical level (e.g., a Car-Parinello type of quantum mechanical dynamics) in a water bath would be necessary in order to appreciate the radial distribution functions and residence time of the water molecules around the base. This kind of analysis will presumably enable us to estimate the lifetime associated with each of the suitable configurations in an aqueous medium, suggested either by the present investigation or by other analyses on this topic.[25,26]

Acknowledgment. The authors thank IDRIS-CNRS (Orsay, France), CINES (Montpellier, France), and CCR (Jussieu, Paris, France) calculation centers for the computational facilities on NEC SX5, IBM Power2, and IBM Power3, respectively. We thank C. Kadri and H. Ismaël for their help in performing some numerical calculations.

References and Notes

(1) Saenger, W. *Principles of Nucleic Acid Structure*, Cantor; C. R., Ed., Springer-Verlag: New York 1984.
(2) Jeffrey, G. A.; Saenger, W. *Hydrogen Bonding in Biological Structures*, Springer-Verlag: New York 1991.
(3) Westhof, E. Water: An integral part of nucleic acid structure; *Annu. Rev. Biophys. Biophys. Chem.*, **1988**, *17*, 25.
(4) Westhof, E.; Beveridge, D. L. Hydration of nucleic acids; *Water Sci. Rev.*; **1990**, *5*, 24.
(5) Berman, H. M.; Schneider, B. Nucleic acid hydration in *Oxford Handbook of Nucleic Acid Structure*, Neidle, S., Ed.; Oxford University Press: New York, 1999; Chapter 9, p 295.
(6) Schneider, B.; Cohen, D.; Berman, H. M. *Biopolymers* **1992**, *32*, 725.
(7) Guéron, M.; Kochoyan, M.; Leroy, J. L. *Nature* **1987**, *328*, 89.
(8) Leroy, J. L.; Kochoyan, M.; Huynh-Dinh, T.; Guéron, M. *J. Mol. Biol.* **1988**, *200*, 223.
(9) Varani, G.; Cheong, C.; Tinoco, I., Jr. *Biochemistry* **1991**, *30*, 3280.
(10) Varani, G. *Annu. Rev. Biophys. Biomol. Struct.* **1995**, *24*, 379.
(11) Jucker, F. M.; Heus, H. A.; Yip, P. F.; Moors, E. H. M.; Pardi, A. *J. Mol. Biol.* **1996**, *264*, 968.
(12) Jucker, F. M.; Pardi, A. *Biochemistry* **1995**, *34*, 14416.
(13) Desiraju, G. R. *Acc. Chem. Res.* **1996**, *29*, 441.
(14) Wahl, M. C.; Sundaralingam, M. *Trends Biochem. Sci.* **1997**, *22*, 97.
(15) Auffinger, P.; Westhof, E. *J. Mol. Biol.* **1997**, *274*, 54.
(16) Pullman, A.; Perahia, D. *Theor. Chim. Acta* **1978**, *48*, 29.
(17) Smets, J.; McCarthy, W. J.; Adamowicz, L. *J. Phys. Chem.* **1996**, *100*, 14655.
(18) van Mourik, T.; Price, S. L.; Clary, D. C. *J. Phys. Chem. A.* **1999**, *103*, 1611.
(19) van Mourik, T.; Benoit, D. M.; Price, S. L.; Clary, D. C. *Phys. Chem. Chem. Phys.* **2000**, *2*, 1281.
(20) Nguyen, M. T.; Chandra, A. K.; Zeegers-Huyskens, Th. *J. Chem. Soc., Fraday Trans.* **1998**, *94*, 1277.
(21) Chandra, A. K.; Nguyen, M. T.; Zeegers-Huyskens, Th. *J. Phys. Chem. A.* **1998**, *102*, 6010.
(22) Dolgounitcheva, O.; Zakrzewski, V. G.; Ortiz, J. V. *J. Phys. Chem. A* **1999**, *103*, 7912.
(23) Ghomi, M.; Aamouche, A.; Cadioli, B.; Berthier, G.; Grajcar, L.; Baron, M. H. *J. Mol. Struct.* **1997**, *411*, 323.
(24) Aamouche, A.; Berthier, G.; Cadioli, B.; Gallinella, E.; Ghomi, M. *J. Mol. Struct. (THEOCHEM)* **1998**, *426*, 307.
(25) Smets, J.; Smith, D. M. A.; Elkadi, Y.; Adamowicz, L. *J. Phys. Chem. A* **1997**, *101*, 9152.
(26) Gadre, S. R.; Babu, K.; Rendell, A. P. *J. Phys. Chem. A.* **2000**, *104*, 8976.

(27) Aamouche, A.; Ghomi, M.; Coulombeau, C.; Jobic, H.; Grajcar, L.; Baron, M. H.; Baumruk, V.; Turpin, P. Y.; Henriet, C.; Berthier, G. *J. Phys. Chem.* **1996**, *100*, 5224.

(28) Aamouche, A.; Ghomi, M.; Coulombeau, C.; Grajcar, L.; Baron, M. H.; Jobic, H.; Berthier, G. *J. Phys. Chem. A* **1997**, *101*, 1801.

(29) Aamouche, A.; Ghomi, M.; Grajcar, L.; Baron, M. H.; Romain, F.; Baumruk, V.; Stepánek, J.; Coulombeau, C.; Jobic, H.; Berthier,G. *J. Phys. Chem. A* **1997**, *101*, 10063.

(30) Leulliot, N.; Ghomi, M.; Scalmani, G.; Berthier, G. *J. Phys. Chem. A* **1999**, *103*, 9716.

(31) Leulliot, N.; Ghomi, M.; Jobic, H.; Bouloussa, O.; Baumruk, V.; Coulombeau, C. *J. Phys. Chem. B* **1999**, *103*, 10934.

(32) Hocquet, A.; Leulliot, N.; Ghomi, M. *J. Phys. Chem. B* **2000**, *104*, 4560.

(33) Gaigeot, M. P.; Leulliot, N.; Ghomi, M.; Jobic, H.; Bouloussa, O.; Coulombeau, C. *Chem. Phys.* **2000**, *261*, 217.

(34) Frisch, M. J.; Trucks, G. W.; Schlegel, H. B.; Scuseria, G. E.; Robb, M. A.; Cheeseman, J. R.; Zakrzewski, V. G.; Montgomery Jr., J. A.; Stratmann, R. E.; Burant, J. C.; Dapprich, S.; Millam, J. M.; Daniels, A. D.; Kudin, K. N.; Strain, M. C.; Farkas, O.; Tomasi, J.; Barone, V.; Cossi, M.; Cammi, R.; Mennucci, B.; Pomelli, C.; Adamo, C.; Clifford, S.; Ochterski, J.; Petersson, G. A.; Ayala, P. Y.; Cui, Q.; Morokuma, K.; Malick, D. K.; Rabuck, A. D.; Raghavachari, K.; Foresman, J. B.; Cioslowski, J.; Ortiz, J. V.; Stefanov, B. B.; Liu, G.; Liashenko, A.; Piskorz, P.; Komaromi, I.; Gomperts, R.; Martin, R. L.; Fox, D. J.; Keith, T.; Al-Laham, M. A.; Peng, C. Y.; Nanayakkara, A.; Gonzalez, C.; Challacombe, M.; Gill, P. M. W.; Johnson, B.; Chen, W.; Wong, M. W.; Andres, J. L.; Gonzalez, C.; Head-Gordon, M.; Replogle, E. S.; Pople, J. A. Gaussian, Inc.: Pittsburgh, PA, 1998.

(35) Becke, A. D. *J. Chem. Phys. A* **1993**, *98*, 5648. Miehlich, B.; Savin, A.; Stoll, H.; Preuss, H. *Chem. Phys. Lett.* **1989**, *157*, 200. Lee, C.; Yang, W.; Parr, R. G. *Phys. Rev. B* **1988**, *37*, 785. Vosko, S. H.; Wilk, L.; Nusair, M. *Can. J. Phys*. **1980**, *58*, 1200.

(36) Boys, S. F.; Bernardi, F. *Mol. Phys.* **1970**, *19*, 553.

(37) Kestner, N. R.; Combariza, J. E. *Reviews in computational chemistry*; Lipkowitz, K. B.; Boyd, D. B., Eds.; Wiley-VCH: New York; Vol 13, p 99.

(38) Stewart, R. F.; Jensen, L. H. *Acta Crystallogr.* **1967**, *23*, 1102.

(39) Ferenczy, G.; Harsanyi, L.; Rozsondai, B.; Hargittai, I. *J. Mol. Struct.* **1986**, *140*, 71.

(40) Kim, K.; Jordan, K. D. *J. Phys. Chem.* **1994**, *98*, 10089.

(41) Odutola, J. A.; Dyke, T. R. *J. Chem. Phys.* **1980**, *72*, 5062.

(42) Scherer, J. R. In *Advances in infrared and Raman spectroscopy*; Clark, R. J. H., Hester, R. E., Eds.; Heyden: New York, 1978; Vol. 5.

(43) Curtis, L. A.; Frurip, D. J.; Blander, M. *J. Chem. Phys.* **1979**, *71*, 2703.

(44) Nunziante-Cesaro, S.; unpublished results as quoted in Harzànyi, L.; Csàszàr, P.; Csàszàr, A.; Boggs, J. E. *Int. J. Quantum Chem.* **1986**, *29*, 799. Bardi, G.; Bensivenni, L.; Ferro, D.; Martini, B.; Nunziante-Cesaro; Teghil, R. *Thermochim. Acta* **1980**, *40*, 275.

(45) Les, A.; Adamowicz, L.; Nowak, M. J.; Lapinski, L. *Spectrochim. Acta* **1992**, *48A*, 1385.

(46) Tursi, A. J.; Nixon, E. R. *J. Chem. Phys.* **1970**, *52*, 1521.

(47) Ayers, G. P.; Pullin, A. D. E. *Spectrochim. Acta* **1976**, *23A*, 1641.

(48) Gaigeot, M. P.; Kadri, C.; Ghomi, M. *J. Mol. Struct.* **2001**, *565-566*, 469.